Icarus **155**, 324–339 (2002)
doi:10.1006/icar.2001.6735, available online at http://www.idealibrary.com on IDEAL®

Related Magma–Ice Interactions: Possible Origins of Chasmata, Chaos, and Surface Materials in Xanthe, Margaritifer, and Meridiani Terrae, Mars

M. G. Chapman and K. L. Tanaka

U.S. Geological Survey, 2255 N. Gemini Drive, Flagstaff, Arizona 86001
E-mail: mchapman@usgs.gov

Received November 6, 2000; revised July 29, 2001

We examine here the close spatial and temporal associations among several unique features of Xanthe and Margaritifer Terrae, specifically the Valles Marineris troughs or chasmata and their interior deposits, chaotic terrain, the circum-Chryse outflow channels, and the subdued cratered material that covers Xanthe, Margaritifer, and Meridiani Terrae. Though previous hypotheses have attempted to explain the origin of individual features or subsets of these, we suggest that they may all be related. All of these features taken together present a consistent scenario that includes the processes of sub-ice volcanism and other magma/ice interactions, results of intrusive events during Late Noachian to Early Amazonian times.

Key Words: **Mars; volcanism; chasmata; tuya; jökulhlaup.**

INTRODUCTION

Xanthe and Margaritifer Terrae contain the circum-Chryse outflow channels and their trough (chasmata) and chaos sources (Fig. 1). The geologic history of the region is complex. At Xanthe and Margaritifer Terrae and directly east in northern Terra Meridiani, ancient highland cratered material is overlain by the subdued cratered unit previously interpreted to be of Late Noachian age (Scott and Tanaka 1986, Greeley and Guest 1987, Witbeck *et al*. 1991, Rotto and Tanaka 1995; Fig. 1). This material and all other units (of Hesperian and Noachian age) adjacent to the chasmata were modified by disruption incurred during the formation of the Valles Marineris chasmata and later eroded by the outflow channels (Scott and Tanaka 1986, Witbeck *et al*. 1991, Rotto and Tanaka 1995).

The chasmata that compose the Valles Marineris on Mars form the largest array of interconnected canyons in the Solar System, over 3200 km in length. The troughs, which range from 50 to 600 km wide, are interconnected and 2- or 3-sided, except for the enclosed Hebes Chasma (Fig. 1). The chasmata lie on a regional high extending westward toward the Tharsis rise (Smith *et al*. 1999), and they are paralleled by many shallow grabens that are part of a system radial to the Tharsis rise (Carr 1974, Wise *et al*. 1979, Plescia and Saunders 1982). Areas of Ophir, Candor, Melas, Hebes, Gangis, Juventae, and Tithonium Chasmata are partly filled in places with Late Hesperian and Amazonian interior deposits forming mesas and benches (McCauley 1978, Witbeck *et al*. 1991).

Xanthe and Margaritifer Terrae are also noted for their topographic basins and ancient valley networks (Grant 1998) and large areas of chaotic or disrupted terrains (Saunders 1979; Fig. 1). Chaotic terrains are generally oval, elliptical, or subcircular in shape; some areas are confined to possible ancient impact craters. Originating at both the chaos and the chasmata are the immense outflow channels that appear to have been cut in the Late Hesperian to Early Amazonian age (Scott and Tanaka 1986, Chapman and Scott 1989, Witbeck *et al*. 1991, Rotto and Tanaka 1995).

The treatise of this paper is that all of the unique features of Xanthe and Margaritifer Terrae may be interrelated. In support of this treatise is the Mars Global Surveyor (MGS) Thermal Emission Spectrometer (TES) discovery of concentrations of crystalline hematite within the chasmata, chaos, and subdued material of Meridiani, Xanthe, and Margaritifer Terrae (Christensen *et al*. 1998, 2000a, 2001, Noreen *et al*. 2000). Perhaps the chasmata, chaotic terrains, interior deposits, outflow channels, and subdued crater material occur together in this locale because they all relate to and have been formed by magma–ice interactions during intrusive events that correspond to peak periods of Tharsis activity. In this paper, these features and their geologic relations will be discussed in detail. While each item taken individually is not evidence of a singular origin, taken collectively they present a unique scenario that suggests volcanism and ice. That the features in question are interrelated is consistent with the evidence we present, but by no means proof positive that they have a singular origin. Thus this paper merely presents a valid hypothesis to be evaluated and weighed along with many others.

OUTFLOW SOURCES: FORMED BY NEAR-SURFACE INTRUSIONS

The chasmata are elongated along a NW–SE axis. Kasei, Maja, and other outflow channels can be traced to eastern Valles Marineris and Echus, Hebes, Juventae, and Gangis Chasmata

0019-1035/02 $35.00

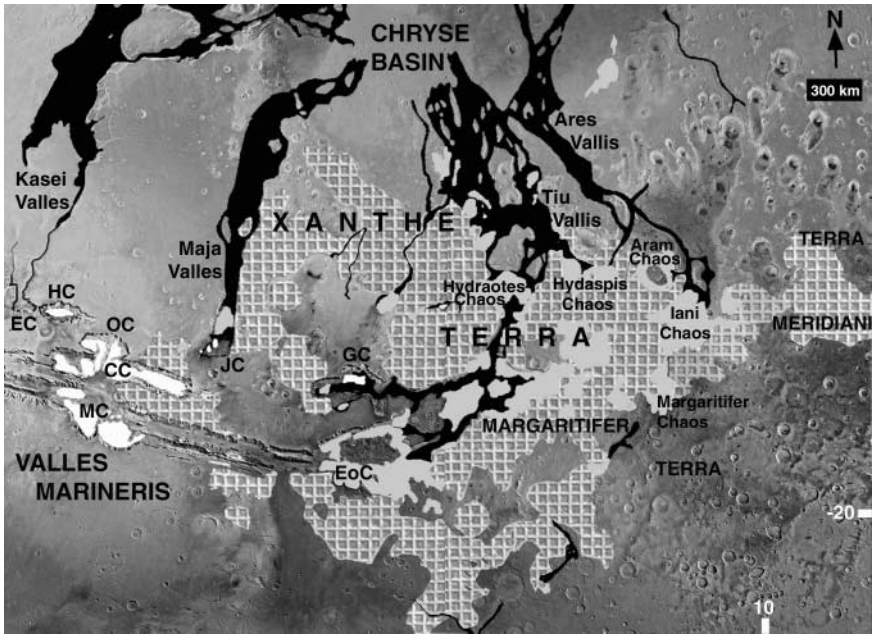

FIG. 1. Location map showing Valles Marineris troughs (EC = Echus Chasma, HC = Hebes Chasma, OC = Ophir Chasma, CC = Candor Chasma, MC = Melas Chasma, JC = Juventae Chasma, GC = Gangis Chasma, and EoC = Eos Chasma), Chryse Basin, and Xanthe, Margaritifer, and Meridiani Terrae; outflow channels shown in black; interior deposits shown in white; chaos shown in grey; subdued cratered unit shown patterned.

(Fig. 1). The Valles Marineris troughs have been generally interpreted as large grabens and (or) collapse structures, produced in association with tensional stresses generated by the Tharsis rise during the Late Noachian to Early Hesperian age (Scott and Tanaka 1986, Witbeck *et al*. 1991, Lucchitta *et al*. 1992). Dynamic upwarping and rising magma caused by a local mantle plume may account for structures at Valles Marineris (Hartmann 1973, Carr 1974, Wise *et al*. 1979, Chapman and Tanaka 2000).

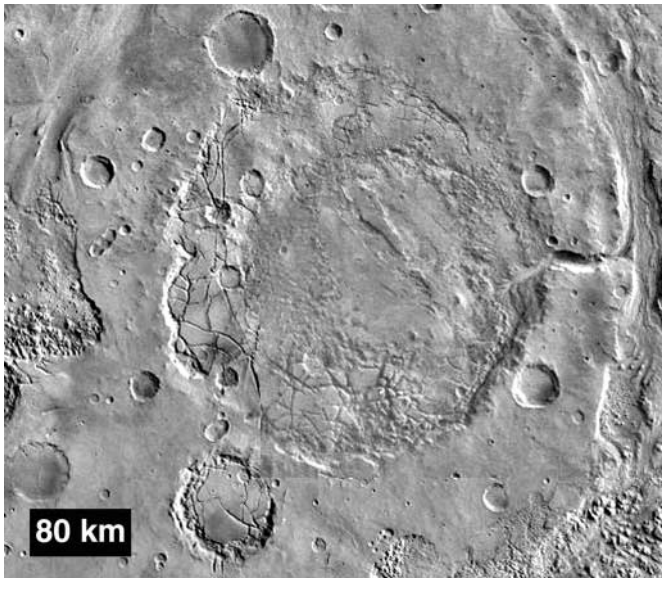

FIG. 2. Viking mosaic centered on Aram Chaos; part of Hydaspis Chaos on the left; location shown in Fig. 1.

Maja and Tiu Valles have both chasmata and chaotic terrain sources. Other circum-Chryse channels have only chaotic sources; an example is Ares Valles, sourced by Aram, Hydaspis, Iani, and Margaritifer Chaos (Fig. 1). Chaos consists of jumbled and subsided blocks of material that may be explained by collapse of overlying rocks due to the melting of ground ice and expulsion of ground water and rock debris (Fig. 2; Sharp 1973, Saunders 1979, Komatsu *et al*. 2000). Magmatic intrusion could have provided the energy for the melting (Masursky *et al*. 1977, Max and Clifford 2000). Eruption and drainage of magma may have contributed to chaos subsidence (Sharp 1973) and may have utilized fractures formed by previous impacts. Although other scenarios for the formation of chaos are just as likely, an eruptive origin for some chaotic terrains is consistent with the tenuous identification of nested collapse pits with possible maar/tuff cone rims on the northeast wall of Hydraotes Chaos (Fig. 3) and the occurrence of concentrated crystalline hematite within dark materials of Aram Chaos (Noreen *et al*. 2000). In addition, other workers have suggested that magmatic intrusions could have mobilized subsurface CO_2 ice leading to eruption of the gas, chaotic collapse, and cryoclastic mass flows with extreme runouts (Hoffman 2000, Tanaka *et al*. 2001).

INTERIOR DEPOSITS: SUB-ICE VOLCANOES

In many areas the interior deposits stand alone, separated from the chasmata walls by a moat, giving them the appearance of having been eroded, down-faulted, or collapsed back from their original extent (Fig. 4; Blasius *et al*. 1977). Commonly a massive section of fluted rocks occurs at the base of these deposits,

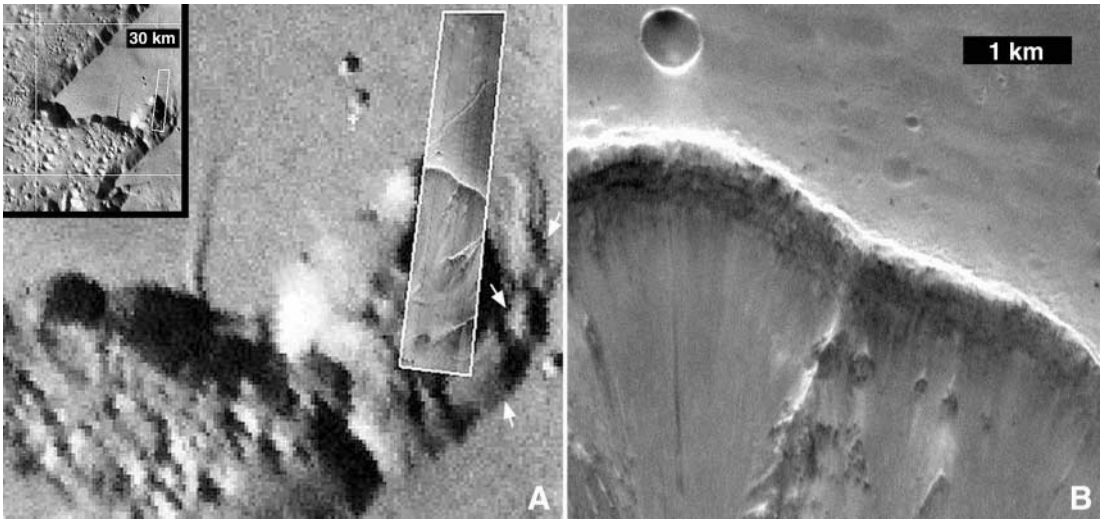

FIG. 3. (A) Viking context image showing part of east wall of Hydraotes Chaos (black inset box); white arrows point to nested pits; white inset box shows Mars Orbital Camera (MOC) image 08805 (5.34 m/p). (B) Enlargement of part of MOC image showing raised rim.

likely scoured by eolian erosion (Breed *et al*. 1983). Overlying the fluted material are layered materials composed of beds of varying thickness; rhythmic broad dark and light albedo bands are locally present on Viking images (Lucchitta *et al*. 1992); however, MOC shows many of these dark bands to be eolian dunes that collect on benches. On many mesas, in Ophir, Candor, and Melas Chasmata, a particularly resistant material forms a caprock above the layered unit and may consist of volcanic materials or a cemented sedimentary unit (Lucchitta 1999).

Previously suggested origins for the layered interior deposits include: aeolian deposits (Peterson 1981), wall debris (Nedell *et al*. 1987), volcanic material (Peterson 1981, Lucchitta, 1981, 1990, Weitz 1999), and lacustrine deposits (McCauley 1978, Carr 1981, Peterson 1981, Lucchitta, 1982, Nedell 1987, Weitz and Parker 2000, Malin and Edgett 2000). Lucchitta (1982), Nedell *et al*. (1987), and Lucchitta *et al*. (1992) discussed these possibilities and concluded that the deposition of the layered deposits in standing bodies of water may best explain the location, apparent near horizontality of many layers, lateral continuity, great thickness, and stratigraphic relations with other units within Ophir, Melas, and Candor Chasmata.

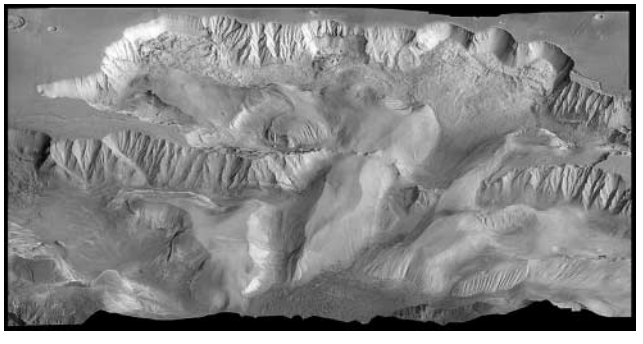

FIG. 4. Oblique view of Ophir and Central Candor Chasmata within Valles Marineris, showing interior deposit mesas; Ophir Chasma is approximately 300 km long, 180 km wide, and 5 km deep; location shown in Fig. 1.

Although deposition in standing water could account for some characteristics of interior deposits, the lacustrine hypothesis was noted to be deficient (Peterson 1981, Lucchitta *et al*. 1992). For example: (1) no large channels that might have supplied the massive amount of sediments are seen to drain into the troughs (Lucchitta 1990); (2) a lake in the connected chasmata cannot explain the local moats that separate some of the deposits from the trough walls; (3) lake beds could not form the angled beds that occur on some mound flanks (Chapman and Tanaka 2001); and (4) a lacustrine origin cannot account for the selectively occurring resistant caprock, which is present on some but not all adjacent mesas of similar height in the interconnected Ophir, Candor, and Melas Chasmata. Ancient terrestrial lake deposits usually contain cyclical sequences of trangressive–regressive facies (Eugster and Surdam 1973, Eugster and Hardie 1975), and these are not observed in the interior deposits by MOC. Instead, Komatsu *et al*. (1993) observe adjacent mounds with distinctly different morphologies, suggesting variable depositional histories for individual mounds—an impossible scenario for lacustrine materials. Moreover, typical lacustrine minerals such as carbonates and other evaporites have not been detected in Valles Marineris by the Thermal Emission Spectrometer (TES). Instead, this site yields a basaltic spectrum (Christensen *et al*. 1998), with some lower concentration of andesite (Bandfield *et al*. 2000).

Others have noted that a volcanic origin for the interior deposits is supported by the regional volcano–tectonic setting of Valles Marineris, tuff-like weathering of layers, and the occurrence of dark materials in the chasmata, and is consistent with the layer diversity and the low albedo and high competence of some layers (Peterson 1981, Geissler *et al*. 1990, Lucchitta 1990, Witbeck *et al*. 1991, Weitz 1999). Whereas Nedell *et al*.

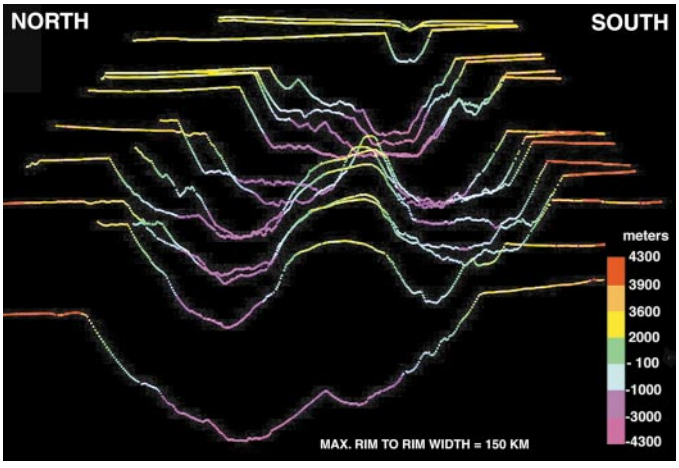

FIG. 5. MOLA profiles across Hebes Chasma, looking east. Hebes Chasma is approximately 300 km wide; location shown in Fig. 1.

(1987) cited a lack of volcanic craters within Valles Marineris, they acknowledged that subaqueous eruptions might have buried such vents. Later, Lucchitta (1990, 1999) showed some irregular depressions that could be calderas.

Recently, we have interpreted the interior deposits to be sub-ice volcanoes based on their dimensions, morphologies, and associated catastrophic floods and other geologic events (Chapman and Tanaka 2001). We contend that sub-ice eruptions are consistent with all of the previous observations (see Table 1 in Chapman and Tanaka 2001), as these eruptions form unstable temporary lakes and result in volcanoes, mostly formed in a lacustrine environment. On Earth, these eruptions are initially overlain by ice, subsequently followed by meltwater (derived from ice by volcanic heat) overlain by an ice cupola. If the pile emerges from the meltwater as an englacial (en-ice) lake (the cupula melts away), a resistant caprock may be emplaced, resulting in a tuya (Van Bemmelen and Rutten 1955, Chapman *et al*. 2000). Tuyas generally have three main constituents, in the following general stratigraphic order: (1) pillow lava, (2) layered and massive hyalotuffs (highly vesicular, altered, and compacted glass shards) and hyaloclastites, overlain by (3) resistant lava (Van Bemmelen and Rutten 1955). Sub-ice pillow lava resembles normal suboceanic pillows, except that they are riddled by cooling joints causing them to be highly friable (Van Bemmelen and Rutten 1955). Effusion of pillow lava gradually transitions to explosive eruptions resulting in hyalotuffs because of changes in (1) the volatile content of the magma and (2) the hydrostatic pressure of the overlying water column above the vent (Jones, 1970, Kokelaar 1986). As the hyalotuff pile grows, it mantles and may conceal the underlying pillow lava mound, unless, during the construction of a volcano, the water height increases and pillows form again. Volcanic heat and ample water in the surrounding meltwater lake cause rapid palagonite alteration in variable degrees (Fisher and Schmincke 1984, Chapman *et al*. 2000). Subaerial lava flows form a caprock. Finally, continued eruption may form highly erodible cinder cones above the caprock; these may not be preserved.

The particularly resistant material that caps some Valles Marineris mesas may be subaerial lava (Chapman and Tanaka 2001). Although many processes could form resistant rock, this origin could account for the selective occurrence of the caprock, as individual volcanoes form at different rates and times (ice levels may vary); some may not reach the meltwater boundary to form caprock. Supporting the interpretation of a sub-ice volcanic origin are the near-infrared spectral data from the ISM (imaging spectrometer for Mars) instrument on board Phobos 2

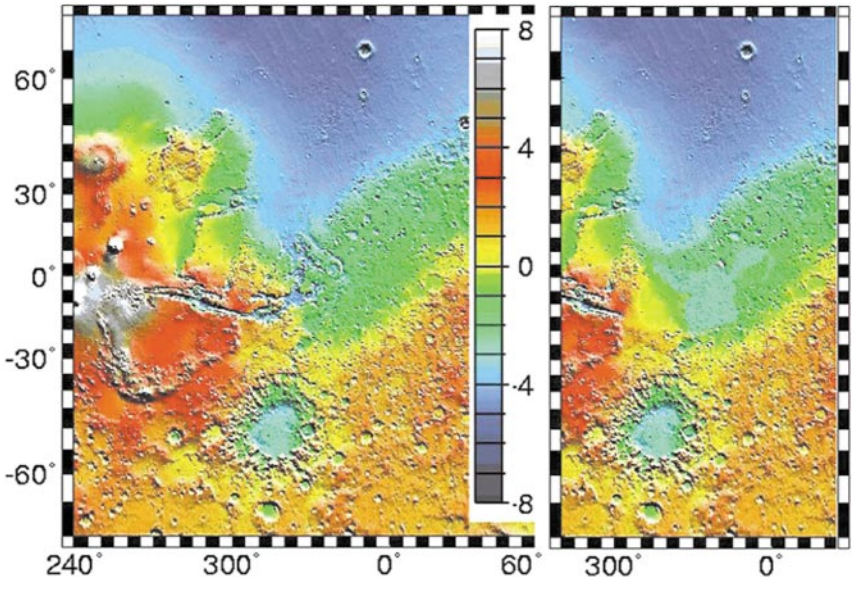

FIG. 13. On left, MOLA topography of area encompassing that of Fig. 1; on right, figure showing inferred location of possible Late Noachian predepositional basin beneath the subdued cratered unit; adapted from Smith *et al*. 1999.

that indicate the interior mounds are highly water-altered palagonitic rocks (Murchie *et al*. 2000). Although a tuya origin would require very thick ice sheets in the chasmata, it would be a much smaller water volume than that called for by a lacustrine origin, as water/ice levels would be below the putative-subaerial-lava caps of resistant material (Chapman and Tanaka 2001). The interior deposits are an order of magnitude larger than terrestrial tuyas, which are limited by the volume of their ice sheets. However, many interior mounds are smaller than Hawaiian volcanoes and there are no terrestrial ponds that can compete with the volume of Valles Marineris (Chapman and Tanaka 2001). Assuming sufficient magma and ice supply, the difference in scale between the terrestrial and martian landforms likely has no bearing on whether the Mars features might be volcanic.

Some of the best-exposed interior deposits may be in Hebes Chasma. Because they are relatively thick (Nedell *et al*. 1987), talus deposits do not cover them (Peterson 1981) and no outflow channels with eroding fluids occur (Chapman and Tanaka 2001). There, Mars orbiter laser altimeter (MOLA) data show about a 4-km-high deposit, whose top rivals the surrounding plateau in elevation (Fig. 5; Chapman and Tanaka 2000). In addition, MOLA data show one mesa in east Candor Chasma (lat. 8.1°S., long. 65.8°) that also rivals the level of the plateau height. Therefore, the uppermost deposits are likely not lacustrine, as lake deposits rarely reach brim full height (Malin 1976, Chapman and Tanaka 2000). MOLA topography and MOC imagery indicate that the Hebes, Ophir, and Candor deposits have the distinctive flat-topped, table morphology of a tuya (Fig. 5; see plate 1, Figs. 7 and 8 in Chapman and Tanaka 2001). Lucchitta *et al*. (1994) previously noted the similarity of the flat-topped morphology of interior deposits in Gangis and Juventae Chasmata to tuyas as well. The morphology of Icelandic tuyas are described and illustrated at length by Van Bemmelen and Rutten (1955). Croft (1990) suggested that the Hebes layers bear an uncanny erosional resemblance to those of Icelandic hyaloclastic mounds (uncapped sub-ice volcanoes) like Sellandafjall, in that both have wall fluting, variable albedo layering, and a soft cap deposit, with no obvious volcanic vents. In addition, free-standing volcanoes can account for the local moats that separate some of the deposits from the trough walls and the layers that dip down at mound peripheries (Chapman and Tanaka 2001).

OUTFLOW CHANNELS: CARVED BY JÖKULHLAUPS GENERATED BY SUBGLACIAL VOLCANIC ERUPTIONS

The most commonly cited origin for the outflow channels is catastrophic flooding (Baker *et al*. 1992). On Earth, catastrophic floods are formed only by natural or man-made dam bursts or subglacial volcanic eruptions (Baker and Milton 1974). The fact that chasmata lead to outflow channels suggests that these voids held a source of ponded water. If the interior deposits are tuyas and hyaloclastite mounds, then they are evidence of ice within Valles Marineris and an eruption-induced flood origin for some of the outflow channels.

In Iceland, subglacial eruptions produce enough meltwater to float the overlying ice cap; subsequent floods pour down subglacial channels carrying rapidly quenched and shattered basaltic debris (Van Bemmelen and Rutten 1955). When these jökulhlaups debouch from the glaciers, they tear off large blocks of ice and entrain underlying material (Williams and McBirney 1979). As the onrushing floods bulk up with debris they may transition into lahars (volcanic mass flows; Van Bemmelen, 1949) that fan out on the "sandur plains" of southern Iceland and spread into the sea. In a fashion similar to jökulhlaups, catastrophic floods debouching from chasmata and chaotic terrains may have bulked up with eroded material to form mass flows (Tanaka 1997, 1999, Chapman and Kargel 1999). Mass flow deposits in Chryse Planitia are consistent with the large locally imbricated rocks observed at the Pathfinder Site below Tiu and Ares Valles and with the lobate flow fronts in Chryse basin (Fig. 1; Nummedal and Prior 1981, Jöns 1990, Lucchitta 1998, Chapman and Kargel 1999, Nelson and Greeley 1999, Tanaka 1999). Rice (2000) noted that MOC and Pathfinder images show transverse ribs, boulders, pit craters, imbricated rocks, percussion marks, and possible conglomerate, similar to those formed by jökulhlaups on the sandur plains of Iceland. However, these features occur in all catastrophic flood environments.

Mass flows sourced from chaos, while having a volcanic trigger at depth (i.e., elevated heat flow) may not have experienced volcanism at the surface. Magmatic intrustions could have mobilized subsurface CO_2 leading to cryoclastic mass flows with extreme runouts (Hoffman 2000, Tanaka *et al*. 2001). Eruption of subsurface CO_2 would not preclude ice in the Valles Marineris chasmata. A CO_2 aquifer, as modeled by Hoffman (2000), has a basal layer of water that could infill surface voids after CO_2 eruption (N. Hoffman, personal communication, 2001) and freeze. CO_2 eruption, later water filling the chasmata, subsequent ice melting by sub-ice volcanism, and jökulhlaup-induced mass flows could presumably all be due to the continued rise of local magma sources to the surface. Therefore mass flows via the outflow channels may well have been cryoclastic as well as volcaniclastic. If the chaos is formed solely by CO_2 eruption, perhaps magma did not continue to rise to the surface at these locales and water remained in the subsurface.

In Valles Marineris, from central Melas Chasma to Eos Chasma (Fig. 1), MOLA topography indicates a net uphill gradient of 0.03° across 1500 km (from Melas to Eos Chasma; Smith *et al*. 1999). Assuming that this gradient has not been modified by later tectonism or resurfacing, it would have resulted in a 1-km-high barrier to water flowing out to the Chryse channels (Smith *et al*. 1999). Cryoclastic flows can surmount topographic barriers (Hoffman 2000). Alternatively, sub-ice eruptions may have generated jökulhlaups whose direction of flow was controlled by the gradient of an overlying ice sheet in Valles Marineris (Chapman and Tanaka 2000). Upslope flow can occur beneath temperate glaciers because the slope of the bedrock and the slope of the overlying ice surface determine the gravity potential (Paterson 1994, Björnsson 1988). If an ice plug controlled

the flow at Valles Marineris, it would have to have been at least 1.125 km thick.

A similar event occurred in association with the 13-day-long fissure eruption in Gjálp, Vatnajökull, Iceland in October 1996 (Gudmundsson *et al*. 1997, Chapman *et al*. 2000). Significant storage of meltwater did not occur at the eruption site of Gjálp, but rather up the bedrock slope in the Grímsvötn caldera lake for 5 weeks before it was released in a very swift jökulhlaup (Gudmundsson *et al*. 1997).

If the hypothetical ice plug in the Valles Marineris was frozen at its base, the floods may have flowed through ice tunnels (or through uppermost permeable ice zones; Smellie 2000) instead of along the ice–ground interface. Possible glacial scour features are not observed in Viking imagery until the point where the channels exit Maja Valles, Echus and Gangis Chasmata, and the chaotic terrains. Perhaps in the upper reaches of the channels, scour and moraine development is either buried by eolian dunes, did not occur due to flow through ice, or did not become large enough to observe in dark albedo channel/chasmata areas that are covered by mostly low-resolution Viking data. Therefore the channels may be explained by a combination of floods, glaciers, and mass-flow processes (Chapman and Kargel 1999).

Stratigraphic relations and geomorphic features indicate that the Kasei and Maja Valles systems have had at least two episodes of erosion (Neukum and Hiller 1981, Chapman and Scott 1989, Chapman *et al*. 1991, Tanaka and Chapman 1992, Baker 1982, Theilig and Greeley 1979). Some of the major channel surfaces have similar crater densities and may have been active simultaneously, whereas others have distinctly separate ages (Rotto and Tanaka 1995). This pattern of multiple discharge areas active at about the same time, and others repeatedly active, is similar to the eruptive patterns of terrestrial volcanic fields. Terrestrial field evidence suggests repeated drainage and refilling of tuya lakes (Smellie and Skilling 1994, Skilling 1994), which occur typically in unstable, active volcanic regions (Björnsson 1988). This pattern may also argue against cryoclastic flow acting alone, as CO_2 eruption may be a one-time per locale event (N. Hoffman, personal communication, 2001).

SUBDUED CRATERED PLAINS MATERIAL: LATE NOACHIAN, VOLUMINOUS IGNIMBRITES?

In the highland regions of Xanthe, Meridiani, and Margaritifer Terrae (Fig. 1), the subdued cratered material (unit Np12; Scott and Tanaka 1986) has an intermediate albedo and a friable surface appearance and buries large craters. The unit has a superposed crater density, as determined from Viking data, similar to that of Early Hesperian ridged plains, which is depicted as possibly a younger unit and mapped as having a dashed (gradational or uncertain) contact with the subdued cratered unit in south Lunae Planum (Scott and Tanaka 1986, Witbeck *et al*. 1991). North Terra Meridiani is mapped as two Noachian units: the widespread subdued cratered unit and an aerially restricted etched unit (Figs. 6 and 7; Scott and Tanaka 1986, Greeley and Guest 1987). Viking images show that both the subdued and etched units overlie the surrounding Middle Noachian materials

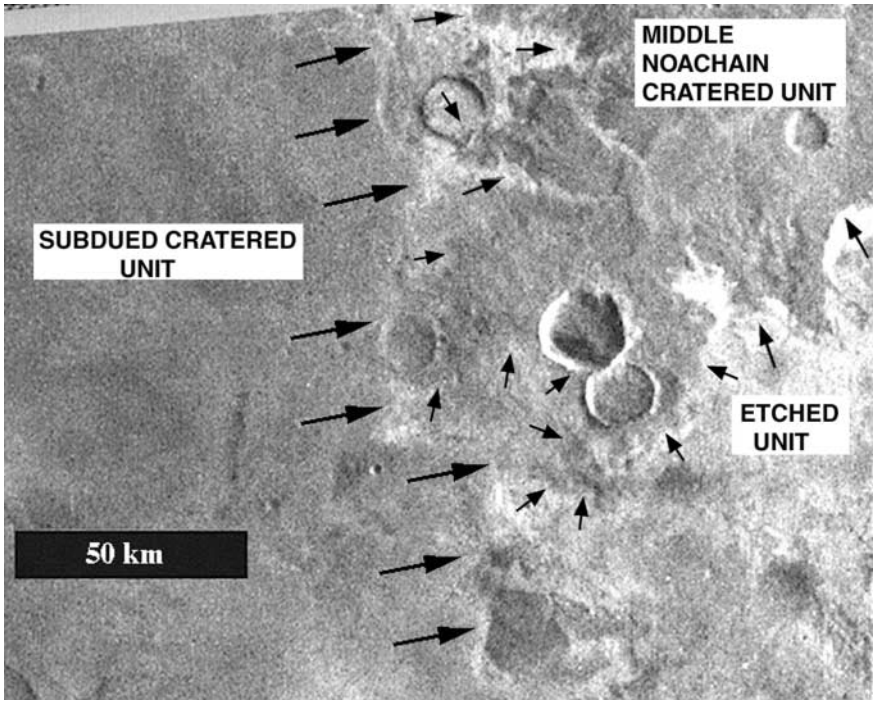

FIG. 6. Viking Orbiter image 655A64 (259 m/p) at about lat. 1.5° N., long. 359° showing erosional contacts of the subdued cratered (large arrows) and etched (small arrows) units; both units overlie the cratered unit of the Middle Noachian age; location shown in Fig. 7.

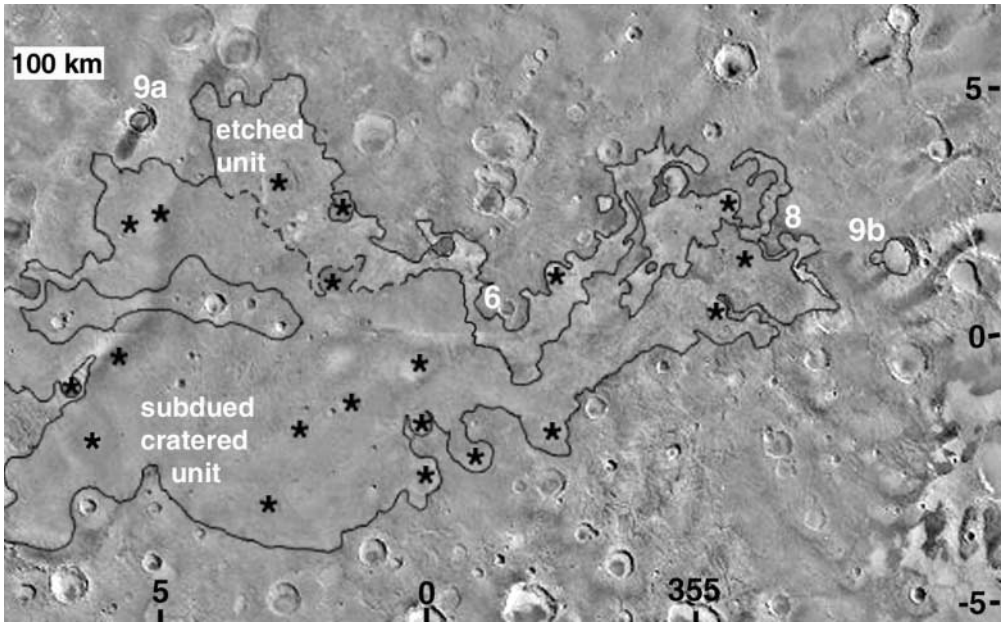

FIG. 7. Viking Mosaic of north Terra Meridiani, showing subdued cratered and etched units; stars mark buried outlines of Noachian impact craters >30 km in diameter, white letters denote location of figures.

(Fig. 6; Chapman 1999a,b, Chapman and Tanaka 2000), as do MOC images (Christensen *et al*. 2000b). In Xanthe and Margaritifer Terrae, the subdued unit is cut by the Late Noachian to Early Hesperian chasmata and by midHesperian age chaotic terrains and outflow channels (Scott and Tanaka 1986, Witbeck *et al*. 1991). The subdued unit's stratigraphic age of Middle to Late Noachian appears to be supported by the somewhat contentious results (see below) from the Viking- and MOC-based crater count data of Terra Meridiani.

The Unit in Terra Meridiani

Viking-based crater counts in Terra Meridiani showed the subdued cratered unit to be comparable in age to the ridged plains of Hesperia, Syrtis Major, Lunae Planum, and south of Hellas (Schultz and Lutz 1988). However, counts from MOC data suggest different ages. Kelsey *et al*. (2000) suggest that densities of small "fossil" craters (250 m to 2 km) indicate a very ancient (4 Ga?) deposit that has been exhumed recently (20–2 Ma?). Hartmann (2001) included the fossil craters and found densities near his saturation equilibrium curve. He concluded that this constrained the surface to have "formed roughly 4 Ga ago," in Noachian time. From the counts of small, fresh craters superimposed on the old features, he proposed an exhumation with "a model age as low as 1 to 40 Ma," formed in Late Amazonian time. The results of counts of small "fossil" craters are curious because they contradict Viking counts of larger craters and because "fossil" craters >2 km have not been observed. Crater counts at MOC resolution which do not include "fossil" craters indicate that the subdued unit in Terra Meridiani is younger than Noachian and may be as young as Amazonian (Gilmore *et al*. 2001). Since Gilmore *et al*. (2001) did not count the subdued "fossil" craters, their results may correspond with Hartmann's estimate of a surface exposed in the Amazonian. Regardless of the cratering ages, the subdued and etched units are both stratigraphically younger than surrounding Middle Noachian units and possibly older than the chasmata, if the subdued unit is truly continuous to Valles Marineris. Because the two units are associated spatially, they may consist of related materials that have very different rock attributes (Chapman 1999a).

In the north Terra Meridiani area, the subdued and etched units nearly bury at least 20 Noachian impact craters about 30 km in diameter (Fig. 7). Using crater rim height/diameter relations for martian craters (Pike 1974, 1977, Garvin *et al*. 2000) and an average crater diameter of 35 km, the combined minimum thickness of the subdued cratered unit and underlying etched unit is about 368 m. This thickness is much less than the 1-km thickness suggested by Schultz and Lutz (1988). The method assumes that the deposit is likely not thick enough to bury craters much larger than 30 km in diameter or we would not see the ghost rims of the smaller 30-km ones.

Viking and MOC images show few impact craters, most <5 km in diameter, superposed on the subdued cratered unit. High-resolution Viking images (25–30 m/p; revs 746A and 408B) show the subdued unit to be smooth. However, MOC images show numerous, small similar-height ridges, a few tens of meters apart, that may not be yardangs or eolian dunes (Edgett and Malin 2000). Many workers have suggested that the subdued unit is some type of friable material, perhaps eroded by wind (Schultz and Lutz 1988, Presley and Arvidson 1988, Edgett and Parker 1997, Chapman 1999a,b, Tanaka 2000, Christensen *et al*. 2000b). Sand-sized material may cover the unit based on

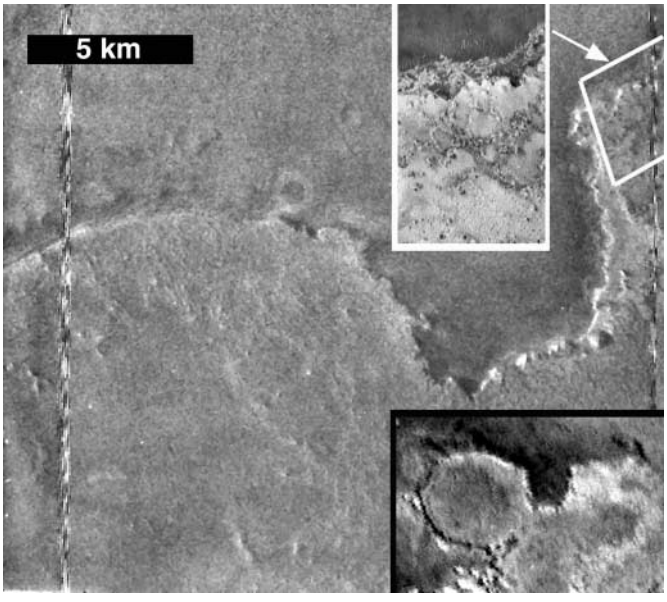

FIG. 8. Viking Orbiter image 709A30 (18 m/p) shows circular rimless mesa, infilled with bright etched unit; black inset box shows part of low-resolution Viking context image; white inset box shows part of MOC image 09003 (5.49 m/p).

fine-component thermal inertia data (221–423 J m^{-2} $s^{-0.5}$ K^{-1}) acquired by Viking (Christensen 1986, Edgett and Parker 1997, Christensen *et al*. 2000b), indicating an average surface particle size equivalent to coarse sand. The unit appears to be layered based on one MOC image (Christensen *et al*. 2000b) and contains the initial hematite area spotted by the TES instrument (Christensen *et al*. 1998), which is associated with the areas of fine ridges (Edgett and Malin 2000).

Northeast of the hematite area, the underlying, somewhat brighter etched unit crops out in a band, as much as 100 km wide, between lat. 0° and 5° N (Fig. 7). The etched unit fills older craters, as does the subdued unit, but not nearly to the same obscuring degree, indicating that it may be thinner. High-resolution Viking images (revs 708A and 709A; 25–28 m/p) show that the etched unit erodes into streamlined knobs, which are likely yardangs. In other areas, this unit has been eroded to expose small, scattered, nonstreamlined mounds or buttes. In several places, the bright etched unit forms perfectly circular mesas, suggesting that it infilled older craters whose rims were later eroded away (Fig. 8). No fluvial features or geomorphic evidence of ground ice is observed. The yardangs and rimless crater fillings indicate that the etched unit is somewhat resistant to erosion. MOC images show that the etched unit is also layered (Christensen *et al*. 2000b).

Many of the large impact craters that bound the subdued and etched units appear to be partly filled with these depositional units. On the west edge of the units, a MOC image shows a bright deposit on the floor of a 30-km-wide impact crater (Fig. 9A). This deposit has long wind-eroded troughs with scattered mounds or buttes among them (Fig. 9A). High-resolution (16 m/p) Viking images also show similar mounds within crater fill on the east edge of the north Terra Meridiani units (Fig. 9B). MOC images show that these types of mounds can also be found elsewhere on outcrops of the etched unit. These mounds and buttes are similar in size and shape to fumarolic mounds formed by vapor escape in terrestrial ignimbrites and in sediments overlying cooling volcanic materials (Chapman 1999a,b). Fumaroles are preferentially cemented in relation to surrounding materials and are exposed when erosion strips away surrounding friable material. The crater fill of Fig. 9B has a lobate termination. Although this appearance may be due to erosion, if it is a primary feature, then the lobe suggests that material flowed up the crater rim to fill its topographic low. The characteristic ability to flow over topographic highs is common to both eolian and ignimbrite

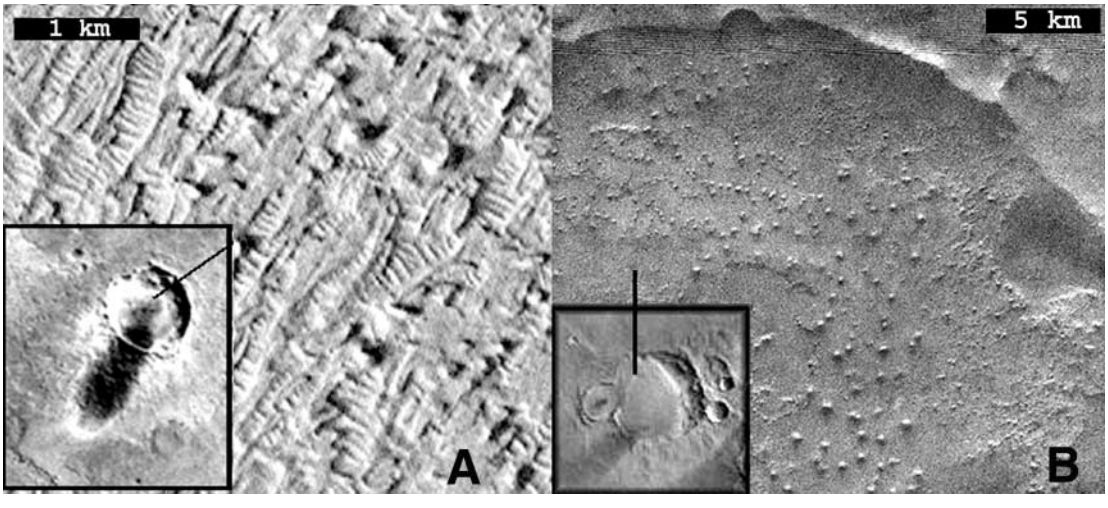

FIG. 9. Scattered mounds or buttes in deposits infilling large craters; location shown in Fig. 7. (A) MOC image 3001 (subframe 3.2 × 3.5 km) shows buttes among long wind-eroded troughs (black inset box shows Viking context image). (B) Viking Orbiter image 709A43 (16 m/p); black inset box shows lobate termination of deposit on Viking context image.

deposits. If eolian, then the sequences have two strikingly different albedos and lithification states; if ignimbritic in composition, then we may be observing zones of differential welding and (or) alteration.

The Unit in Xanthe and Margaritifer Terrae

The outcrops of the subdued crater unit within Xanthe and Margaritifer Terrae are very similar to those of north Terra Meridiani. Although Scott and Tanaka (1986) mapped these areas as distinct outcrops, Rotto and Tanaka (1995) mapped this unit contiguously across all three regions. Based on MOC observations, Malin and Edgett (2000) suggest that the unit is variably layered and continuous from Terra Meridiani to Valles Marineris. In Xanthe Terra, the subdued cratered unit can be observed to fill Noachian craters from 30 to 80 km in diameter to variable depths (Fig. 10). Using crater rim height/diameter relations (Pike 1974, 1977, Garvin *et al*. 2000), the minimum thickness range is found to vary from about 340 to 560 m. The variation in fill depth may be due to heterogeneity in the original depositional thickness or to erosional removal. Wilhelms (1974) argued that the plains, or subdued unit in this region, was depositional and suggested that much of the plains material was perhaps volcanic cover based on its contemporaneous relationship with the wrinkle-ridged plains of Tharsis.

Possible Compositions of the Subdued Unit

TES data indicate a concentration of crystalline hematite within the subdued unit of North Terra Meridiani (Christensen *et al*. 1998) and within Aram Chaos (Christensen *et al*. 2000a, Noreen *et al*. 2000) and Valles Marineris (Noreen *et al*. 2000, Christensen *et al*. 2001) of Xanthe Terra. Xanthe Terra has a basaltic TES spectral signature similar to that of most of the martian southern highlands. However, Margaritifer and Meridiani Terrae display lower concentrations of basaltic andesite to andesite, relative to the high concentrations found in the northern plains (Bandfield *et al*. 2000). Andesitic compositions may be consistent with the interpretation that the subdued unit is tephra material, because this composition is more silicic than basalt. Most geologists are familiar with widespread terrestrial ignimbrites that are silicic (Fisher and Schmincke 1984), although a few are basaltic (Van Bemmelen and Rutten 1955). However, on Earth the basalt/andesite transition has been suggested to be a viscosity barrier in magma, above which large explosive eruptions are possible (Smith 1979, Francis and Wood 1982), and on Mars, even basalts may generate large explosive eruptions (Wilson and Head 1981, 1983). Production of substantial tephra from compositions as mafic as basalt is possible, due to the low-pressure environment on Mars (Wilson and Head 1994, Fagents and Wilson 1996). Perhaps outflow channel erosion removed large amounts of the andesitic subdued unit from Xanthe Terrae, thus depositing the basaltic andesite material in the northern plains. Thus, the andesite (and hematite) in Terra Meridiani may be a relic deposit, undisturbed by catastrophic floods.

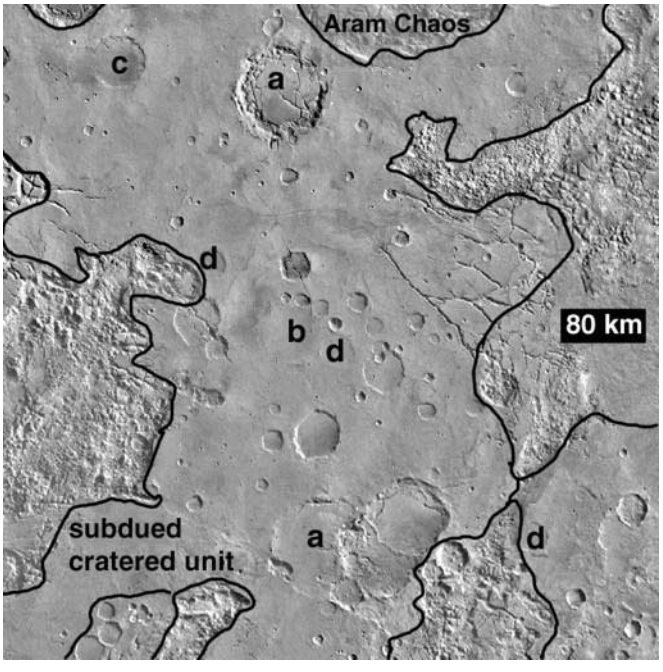

FIG. 10. Viking mosaic showing variable fill of subdued cratered unit in Xanthe Terra; centered at lat. 3°S., long. 22.5°; letters denote diameters of nearly buried craters (a = 80 km, b = 50 km, c = 40 km, d = 30 km).

Possible Origins of the Subdued Unit

Previously, the subdued cratered unit has been interpreted to be thin, interbedded lava flows, eolian material, paleopolar deposits, or water-laid sediments that partly bury underlying rocks, whereas the etched unit has been interpreted to be water-laid sediments (carbonates?) or ancient cratered material degraded by wind erosion, decay of ground ice, and minor fluvial erosion (Scott and Tanaka 1986, Greeley and Guest 1987, Schultz and Lutz 1988, Edgett and Parker 1997, Kelsey *et al*. 2000). Although both units are characterized by layered materials, they lack any other geomorphologic feature that would be diagnostic of origin other than the etched material having bright albedo layers that erode into yardangs. Paleopolar deposits (Schultz 1985, Schultz and Lutz 1988) are doubtful because (1) early buildup of Tharsis makes polar wander unlikely after the Middle Noachian (Tanaka 2000), and (2) the timing of polar wander would require materials (such as the Medusae Fossae Fm.) to be much older than the stratigraphy indicates (Scott and Tanaka 1982). The water-laid sedimentary interpretation is based on (1) the relatively low and flat topography of the area, (2) possible evaporite deposits noted by Lee (1993) within large, old craters, (3) dunes and Viking rock abundance and thermal inertia that indicate sand-sized material, (4) few valley networks, (5) smooth surface of the subdued crater unit, and (6) lack of mantling that would support volcanic or eolian airfall (Edgett and Parker 1997, Malin and Edgett 2000). However, TES has not shown carbonates or evaporites on Mars. Even "white rock," another famous suspected crater-fill

evaporite, lacks spectral evidence for an aqueous origin (Ruff *et al*. 2000).

We would like to suggest an alternative theory of origin, to be evaluated and weighed along with the hypothesis that material is water-laid sediments. It is possible that the andesitic TES signature and other observations, such as layering, scattered mounds, local lobate terminations, and variable albedo, may be more consistent with ignimbrites and ash falls. MOLA topography indicates that the Terra Meridiani deposit occurs on a gentle slope—an unlikely position for lacustrine deposits. While ignimbrites follow preexisting topography and flow into low areas (Fisher and Schmincke 1984), they can mantle slopes. Although sand-sized and larger material obviously can be found in aqueous sediments (Edgett and Parker 1997), these grain sizes are also common to ash flows (Murai 1961, Fisher and Schmincke 1984). Ignimbrites/ash falls would be expected to lack valley networks. Contrary to Viking observations, MOC images show that the unit is not smooth but rather contains numerous fine scale ridges (Edgett and Malin 2000). Mantling is an undiagnostic criterion as airfall, ash flow, and water-laid sediments all form overburden materials that mantle/cover/subdue underlying units. Like the subdued and etched units, ash deposits are layered and have variable albedoes due to compositional changes or differing degrees of alteration.

Formation of the Concentrated Hematite

Christensen *et al*. (2000a,b) have considered five possible mechanisms for the formation of the crystalline hematite: (1) chemical precipitation that includes origins by (a) precipitation from standing, oxygenated, Fe-rich water, (b) precipitation from Fe-rich hydrothermal fluids, (c) low-temperature dissolution and precipitation through mobile groundwater leaching, and (d) formation of surface coatings; and (2) thermal oxidation of magnetite-rich lava. They favor chemical precipitation models involving precipitation from Fe-rich water based on (1) their perceived association of the hematite with lacustrine sedimentary materials (Edgett and Parker 1997), (2) the large geographic area in which hematite has been detected, (3) an apparent large distance of the hematite from regional heat sources, and (4) the lack of evidence for extensive hydrothermal groundwater processes elsewhere on Mars (Christensen *et al*. 2000a). Additional spectral studies suggest that the hematite may be composed of axis-oriented hematite grains, which may occur as metamorphosed, schistose hematite deposits or as very well aligned, platy, discrete hematite particles (Lane *et al*. 2000).

In counterpoint argument to the TES Team's basis for their model, the association of the hematite solely with lacustrine sedimentary material is outdated, as the above discussion notes an alternative to this origin. Secondly, an ash-flow/fall origin for the subdued cratered unit may account for the unit's outcrops across a large geographic area with variable slopes and elevations. Thirdly, crystalline hematite has been found in several locales within the subdued unit—a plains unit associated with chaos and chasmata in Xanthe and Margaritifer Terrae—huge, possible eruptive sites that could have vented widespread ash flows and provided regional heat sources. In addition, hematite occurs well within the chasmata. Finally, possible evidence and influence of volcanism-induced hydrothermal systems on Mars have long been recognized (Schultz *et al*. 1982, Brakenridge *et al*. 1985, Gulick and Baker 1989, 1990). Fe-rich hydrothermal fluids might be generated by volcanic heat from below (Noreen *et al*. 2000). Noreen *et al*. (2000) suggest El Laco, Chile as a possible terrestrial analog site for the martian hematite deposits. Magnetite–hematite deposits on El Laco volcano, Chile, contain copious amounts of primary and secondary hematite associated with andesitic ash flows (Nyström and Henríquez 1994). The deposits are composed of axis-oriented crystals due to flow layering and stratification of erupted material (Nyström and Henríquez 1994). Hematite occurs within the magnetite deposits (Henríquez and Martin 1978). The magnetite bodies are thought to be either primary volcanic flows (Naslund *et al*. 1997, 1998) or to have formed via metasomatic replacement of andesite flows and hydrothermal precipitation (Rhodes *et al*. 1997). Minerals other than hematite have not been observed on the martian deposits (Christensen *et al*. 2000b). Similar to El Laco, perhaps this mineral paucity may be due to primary hematite deposition and/or alteration of primary magnetite grains. Although Catling and Moore (2001) argue that oxygen fugacity values derived from martian meteorites are too low to permit the direct derivation of hematite by volcanism, Shergottite, Nahklite, and Chassignite meteorites, and ALH84001—those suspected to be from Mars—are magmatic basalts and dunites, not andesites. Terrestrial andesites can have higher water contents and elevated oxygen fugacities in relation to basalts and dunites.

To address the argument that the hematite is schistose and originally water-laid (Edgett and Parker 1997), fine-grained, red hematite would need to be recrystallized to coarser, gray hematite through low-grade metamorphism produced by burial with as much as 4 km of material (Lane *et al*. 2000). This overburden would then have to be stripped away, leaving the schistose hematite exposed at the surface of Mars (Lane *et al*. 2000). However, this thickness of overburden would be approximately 4 km higher in elevation than the lacustrine shoreline contact envisioned by Edgett and Parker (1997). Lake sediments cannot be deposited above water line. Alternatively, ignimbrites produce banded, flattened, and aligned shards and crystals (Chapin and Lowell 1979, Peterson 1979), and andesitic ash flows could produce aligned iron-rich crystals such as magnetite that could alter to hematite (Rhodes *et al*. 1997). Eolian winnowing of ash could also secondarily produce aligned minerals.

DISCUSSION

Malin and Edgett (2000) note the layering and albedo similarities between the subdued unit and the interior deposits, their mantling nature, and their lack of large clasts, and suggest that

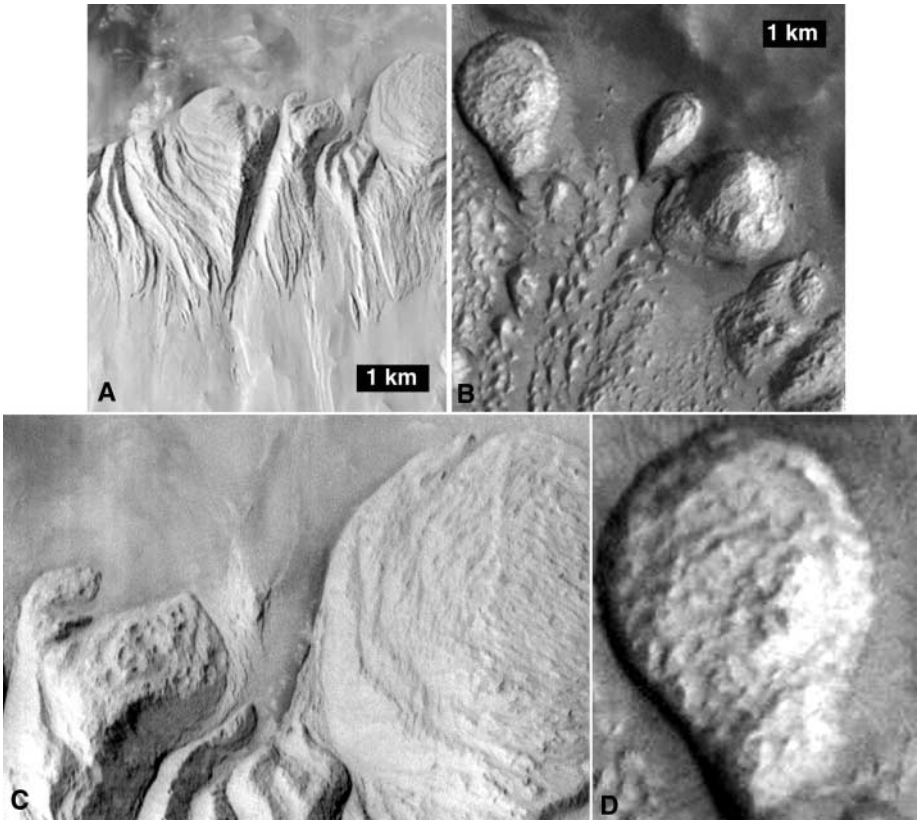

FIG. 11. Comparison MOC images of (A) Ophir Chasma interior deposits at lat. 4°S., long. 72.45° (MOC 08204, 5.33 m/p) and (B) the subdued cratered unit within an impact crater at lat. 11°N., long. 4.3° (MOC 35104, 6.03 m/p). (C) Enlargement of part of (A), and (D) enlargement of part of (B). Note similar rounded weathering pattern of outcrops and pits on surface of (C) and (D).

they are probably rocks of like origin and possibly fine-grained sediments. We concur with this opinion (Chapman and Tanaka 2000) and observe that the lithologies even weather similarly in MOC images (Figs. 11 and 12). Furthermore, most of the friable surface of the subdued unit weathers similarly to other parts of the interior deposits that have been subdivided into smooth units, interpreted to be airfall ash or eolian material (Lucchitta 1999). Malin and Edgett (2000) prefer the hypothesis that the

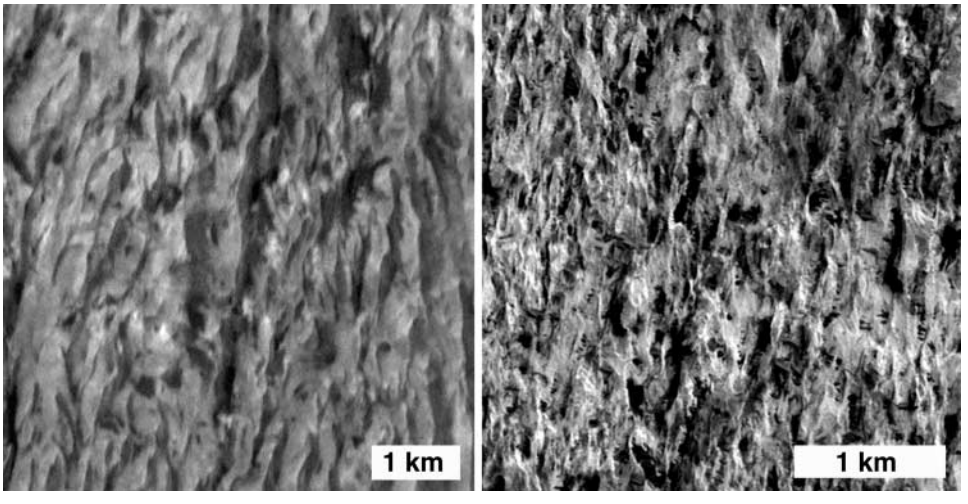

FIG. 12. Similar appearance and weathering pattern of outcrops on MOC images of (A) interior deposits of Gangis Chasma at lat. 7.5°S., long. 49.7° (MOC 08707, 5.44 m/p), (B) the subdued cratered unit at lat. 0.4°N., long. 9.3° (MOC 00740; 2.86 m/p).

material is likely ancient lacustrine rocks. The lacustrine hypothesis requires a large volume of water (often more than the surrounding basin rim height, which the material can overtop) and an ancient age for the stratigraphically young Valles Marineris interior deposits (Chapman 2001). Alternatively, we suggest that perhaps the subdued unit in the plains and the interior deposits in Valles Marineris are composed of ash formed at distinctly different time periods.

A recent examination of TES spectra shows that like Terra Meridiani, some areas of the interior deposits in Valles Marineris and Aram Chaos show high concentrations of crystalline hematite (Noreen *et al*. 2000, Christensen *et al*. 2001). Unlike Terra Meridiani, the Valles Marineris hematite is associated with dark materials (Noreen *et al*. 2000) previously interpreted to be volcanic, and some of the youngest interior materials (Geissler *et al*. 1990, Lucchitta 1990). The hematite mineralization may be due to like processes operating at different times or late-stage alteration of similar morphologies. The latter seems unlikely as mineralization should occur across lithologies rather than being confined to similar-appearing rocks.

We suggest the following historical scenario that may explain the unique features of the Xanthe, Meridiani, and Margaritifer Terrae regions and the possible ash compositions of the subdued unit and interior deposits. The scenario begins in the Middle to Late Noachian age, when the predepositional topography, below the few-hundred-meter-thick subdued cratered unit, must have included a large shallow basin in Xanthe and Margaritifer Terrae connected to another smaller basin in north Terra Meridiani (Fig. 13). As shown on global scale geologic (Scott and Tanaka 1986, Greeley and Guest 1987) and MOLA maps (Smith *et al*. 1999), both basins would have been separated from the northern lowlands by a band of higher elevation Noachian terrain (Fig. 13).

As noted earlier, most proposed origins of the Valles Marineris troughs require initial development beginning in the Late Noachian to Early Hesperian age (Scott and Tanaka 1986, Witbeck *et al*. 1991, Rotto and Tanaka, 1995). Water from subsurface ice in aquifers might encounter rising magma associated with initial volcanism and extension at Valles Marineris and perhaps eastward. (Eruptive sites in the terrae basins could also include buried fissures.) On Earth, such encounters, between meteoric water and fissure-confined magma, create highly explosive eruptions that may produce widespread ignimbrites, which spread like huge aprons over plains (Van Bemmelen and Rutten 1955, Fisher and Schmincke 1984). For example, the Late Pleistocene faulting and fissuring of the midIcelandic depression allowed large amounts of meteoric water to penetrate at a high rate to great depth, contacting rising magma and turbulently mixing to form the basaltic Ytri ignimbrite (Van Bemmelen and Rutten 1955). (Later eruptions from basalt at depth had less opportunity to mix with groundwater and yielded lava; Van Bemmelen and Rutten 1955.) The subdued cratered unit appears to be Middle to Late Noachian in age, dating from about the formation time of initial Valles Marineris troughs/

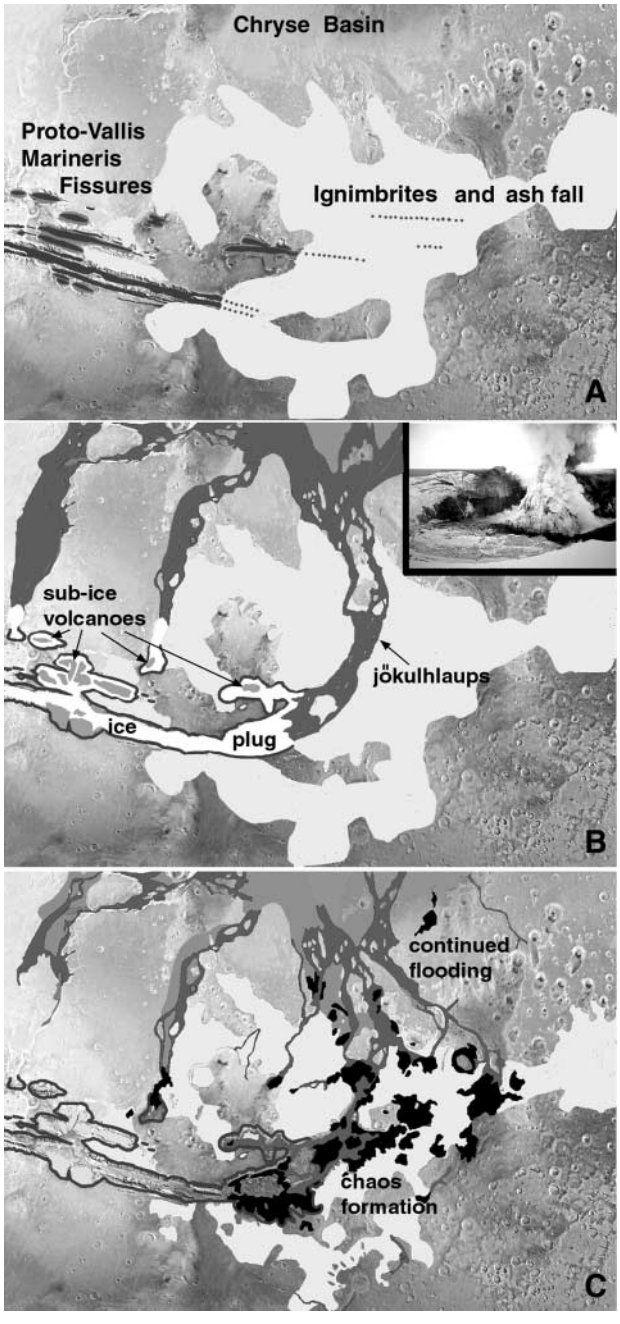

FIG. 14. Hypothetical scenario that accounts for features and materials of Xanthe and Margaritifer Terrae. (A) Fissure eruptions generate ignimbrites that bury ice-rich materials; possible buried fissures indicated by dotted lines. (B) Lava erupted into chasmata ice produces sub-ice volcanoes and floods downstream; inset: Dec. 19, 1998, Grímsvötn subglacial eruption (Oddur Sigurdsson, photographer). (C) Eruptions, beneath ice-rich materials and overlying ash, produce chaos (in black) and continued flooding.

fissures. Ash flows follow general topography and thus would flow downslope away from Valles Marineris toward Xanthe, Margaritifer, and Meridiani Terrae, blanketing the ground ice that had accumulated in the basins (Fig. 14A). Fe-rich

hydrothermal fluids could alter magnetite within the ignimbrites and precipitate hematite at this time.

After these events and later the chaotic areas may have formed. Increased heat flow from rising magna may have melted ground ice (CO_2 and/or H_2O), collapsed the proposed overlying ignimbrite sheet thereby forming areas of chaotic terrain and chasmata, and generated mass flows and floods (Fig. 14C). The associated outflows eroded parts of the subdued cratered unit in Xanthe and Margaritifer Terrae and flowed north into Chryse basin.

The area of the developing Valles Marineris troughs may have become partly filled with water, freed from a confined aquifer (Carr 1979). Alternatively, the water (and some fluvial material) may have been collected within the entire Xanthe/Margaritifer/Meridiani basin region and slowly seeped into the lows of the chasmata, from the south via runoff from overflow of Argyre Planitia (Parker *et al*. 2000) and by subsurface sapping and surface runoff from ancient, small valley systems (Grant 1998). The confined chasmata might continue to fill with groundwater, which would freeze and easily pond in enclosed areas such as Hebes Chasma. Larger ice pondings would also be likely in nonenclosed troughs, as ice on Mars would likely be cold-based (unable to flow) and ignimbrite deposits downslope of the troughs could block their eastward openings. Following most of the trough formation during the Late Hesperian age, the interior deposits were emplaced (Witbeck *et al*. 1991). Similar to the Ytri eruptions, later eruptions from the troughs may have come from basalt at depth, which unable to mix with groundwater, may have yielded lava. Consistent with TES results for a basaltic composition for Hebes deposits (Christensen *et al*. 1998) and near-infrared data from Phobos II that indicate a water-altered palagonite composition for the interior deposits (Murchie *et al*. 2000), this phase may have included the eruption of basaltic lava beneath ponded ice, forming interior tuyas (Chapman and Tanaka 2000; Fig. 14B). Unstable tuya lakes in Echus and Juventae Chasmata could explain the episodic floods at Kasei and Maja Valles. These meltwater lakes could have repeatedly drained via jökulhlaups. Ice plugs in the troughs (Fig. 14B) could explain the uphill drainage out of Valles Marineris. The later volcanism that formed tuyas within Valles Marineris might have occurred eastward as well, in Xanthe and Margaritifer Terrae forming additional chaos. The outflows continued to erode Xanthe Terra. (The hematite of Xanthe Terrae is located in what may have been areas protected from excessive outflow erosion: i.e., the crater of Aram chaos.) After cessation of sub-ice volcanism, any remaining ice in the troughs would have eventually sublimated. Late-stage eruption of dark materials and their subsequent hydrothermal alteration may have formed slightly water-altered mafic (Murchie *et al*. 2000) ash and the hematite in Valles Marineris. Finally, continued tectonism, collapse, and scarp retreat within Valles Marineris may have obliterated some of the earlier landforms related to sub-ice volcanism, and all areas have been heavily eroded by the wind.

CONCLUSION

Xanthe, Meridiani, and Margaritifer Terrae contain the circum-Chryse outflow channels, their chasmata and chaos sources, the interior deposits, and the subdued unit; some surfaces are locally associated with concentrations of crystalline hematite. These unique features and their geologic relations, taken collectively, present a consistent scenario that may suggest volcanism and ice interactions. Magma within the initial Valles Marineris fissures may have encountered water from subsurface ice and exploded violently, producing widespead ignimbrites that blanketed Xanthe, Margaritifer, and Meridiani Terrae and formed the layered subdued plains unit. Later, chasmata and chaos may have formed by near-surface magmatic intrusions. Even later eruptions from the deepening chasmata perhaps yielded lava. This lava may have erupted beneath chasmata-confined cold-based ice, forming interior deposit tuyas and generating jökulhlaups or glacial outwash floods downstream. The floods perhaps eroded and removed large amounts of Xanthe Terra, thus depositing basaltic andesite material in the northern plains. Late-stage eruptions in Valles Marineris could have produced dark ash deposits. Finally, all units have been subject to eolian erosion for eons. The hematite mineralization may be due to late-stage alteration or a combination of ancient and young alteration of volcanic ash by Fe-rich hydrothermal fluids associated with volcanism.

Although this scenario is consistent with the features in question, we can provide no positive proof that it actually occurred. Thus this paper merely presents a valid hypothesis to be evaluated and weighed along with many others. Continued study of MGS data and information from future missions may resolve the origins of outflow channels, chasmata, chaos, the interior deposits, the subdued unit, and concentrations of crystalline hematite.

ACKNOWLEDGMENTS

We are grateful to Jeff Plescia, Jeff Kargel, Rene De Hon, John Grant, and Bill Hartmann for their comments and contributions toward this manuscript. We also thank Eric Noreen for his diligent examination of TES data and for some ideas on hematite formation.

REFERENCES

Baker, V. R. 1982. *The Channels of Mars*. Univ. Texas Press, Austin.

Baker, V. R., and D. J. Milton 1974. Erosion by catastrophic floods on Mars and Earth. *Icarus* **23**, 27–41.

Baker, V. R., M. H. Carr, V. C. Gulick, C. R. Williams, and M. S. Marley 1992. Channel and valley networks. In *Mars* (H. H. Kieffer, B. M. Jakosky, C. W. Snyder, and M. S. Matthews, Eds.), pp. 493–522. Univ. of Arizona Press, Tucson.

Bandfield, J. L., V. E. Hamilton, and P. R. Christensen 2000. A global view of martian surface compositions from MGS–TES. *Science* **287**, 1626–1630.

Björnsson, H. 1988. Hydrology of ice caps in volcanic regions. *Soc. Sci. Islandica* **45**, 137.

Blasius, K. R., J. A. Cutts, J. E. Guest, and H. Masursky 1977. Geology of the Valles Marineris—First analysis of imaging from the Viking 1 Orbiter primary mission. *J. Geophys. Res.* **82**, 4067–4097.

Brakenridge, G. R., H. E. Newsom, and V. R. Baker 1985. Ancient hot springs on Mars: Origins and paleoenvironmental significance of small martian valleys. *Geology* **13**, 859–862.

Breed, C. S., J. F. McCauley, and M. J. Grolier 1983. Multiprocess evolution of landforms in the Kharga region, Egypt—Applications to Mars. *NASA TM* **86246**, 225–227.

Carr, M. H. 1974. Tectonism and volcanism of the Tharsis region of Mars. *J. Geophys. Res.* **79**, 3943–3949.

Carr, M. H. 1979. Formation of martian flood features by release of water from confined aquifers. *J. Geophys. Res.* **84**, 2995–3007.

Carr, M. H. 1981. *The Surface of Mars*. Yale Univ. Press, New Haven, CT.

Catling, D. C., and J. M. Moore 2001. Hematite on Mars and its implications for the early martian environment. *Lunar Planet. Sci.* **32**, 2053 (abstract).

Chapin, C. E., and G. R. Lowell 1979. Primary and secondary flow structures in ash-flow tuffs of the Gribbles Run paleovalley, central Colorado. In *Ash Flow Tuffs* (C. E. Chapin and W. E. Elston, Eds.), pp. 137–154. Geol. Soc. Am. Spec. Paper 180. Geol. Soc. Am., Boulder, Co.

Chapman, M. G. 1999a. 2001 Site in North Terra Meridiani: The TES concentration area. NASA Ames Second Mars Surveyor Landing Site Workshop, Buffalo, New York, June 22–23, 1999 (abstract).

Chapman, M. G. 1999b. Enigmatic terrain of north Terra Meridiani, Mars. *Lunar Planet. Sci.* **30**, 1294 (abstract).

Chapman, M. G. 2001. Layered material of variable albedo on Mars: Possible Late Noachian to Early Amazonian tephra. *Lunar Planet. Sci.* **32**, 1709 (abstract).

Chapman, M. G., and J. S. Kargel 1999. Observations at the Mars Pathfinder site: Do they provide "unequivocal" evidence of catastrophic flooding? *J. Geophys. Res.* **104**, 8671–8678.

Chapman, M. G., and D. H. Scott 1989. Geology and hydrology of the north Kasei Valles area, Mars. *Proc. Lunar Planet. Sci. Conf. 19*, pp. 367–375.

Chapman, M. G., and K. L. Tanaka 2000. Chasmata, chaos, outflow channels, and interior deposits on Mars: Produced by sub-ice eruptions? *Lunar Planet. Sci.* **31**, 1256 (abstract).

Chapman, M. G., and K. L. Tanaka 2001. The interior deposits on Mars: Sub-ice volcanoes? *J. Geophys. Res.* **106**, 10,087–10,100.

Chapman, M. G., H. Masursky, and D. H. Scott 1991. Geologic map of science study area 2, North Kasei Valles, Mars (MTM 25072). U.S. Geol. Surv. Misc. Invest. Series Map I-2107.

Chapman, M. G., C. C. Allen, M. T. Gudmundsson, V. C. Gulick, S. P. Jakobsson, B. K. Lucchitta, I. P. Skilling, and R. B. Waitt 2000. Volcanism and ice interactions on Earth and Mars. In *Deep Oceans to Deep Space: Environmental Effects on Volcanic Eruptions* (T. K. P. Gregg and J. R. Zimbelman, Eds.), pp. 39–74. Plenum, New York.

Christensen, P. R. 1986. The spatial distribution of rocks on Mars. *Icarus* **68**, 217–238.

Christensen, P. R., D. L. Anderson, S. C. Chase, R. T. Clancy, R. N. Clark, B. J. Conrath, H. H. Keiffer, R. O. Kuzmin, M. C. Malin, J. C. Pearl, T. L. Roush, and M. D. Smith 1998. Results from the Mars Global Surveyor Thermal Emission Spectrometer. *Science* **279**, 1692–1698.

Christensen, P. R., M. Malin, D. Morris, J. Bandfield, M. Lane, and K. Edgett 2000a. The distribution of crystalline hematite on Mars from the Thermal Emission Spectrometer: Evidence for liquid water. *Lunar Planet. Sci.* **31**, 1627 (abstract).

Christensen, P. R., and 15 colleagues 2000b. Detection of crystalline hematite mineralization on Mars by the Thermal Emission Spectrometer: Evidence for near-surface water. *J. Geophys. Res.* **105**, 9623–9642.

Christensen, P. R., R. V. Morris, J. L. Bandfield, M. D. Lane, and M. C. Malin 2001. Global mapping of martian hematite mineral deposits: Remnants of water-driven processes on early Mars. *J. Geophys. Res.* **106**, 23,873–23,885.

Croft, S. K. 1990. Geologic map of the Hebes Chasma quadrangle, VM 500K 00077 (abstract). *NASA TM* **4210**, 539–541.

Edgett, K. S., and M. Malin 2000. The new Mars of MGS MOC: Ridged layered geologic unit (they're not dunes). *Lunar Planet. Sci.* **31**, 1057 (abstract).

Edgett, K. S., and T. J. Parker 1997. Water on early Mars: Possible subaqueous sedimentary deposits covering ancient cratered terrain in western Arabia and Sinus Meridiani. *Geophys. Res. Lett.* **24**, 2897–2900.

Eugster, H. P., and L. A. Hardie 1975. Sedimentation in an ancient playa-lake complex: The Wilkens Peak Member of the Green River Formation of Wyoming. *Bull. Geol. Soc. Am.* **86**, 319–334.

Eugster, H. P., and R. C. Surdam 1973. Depositional environment of the Green River Formation of Wyoming: A preliminary report. *Bull. Geol. Soc. Am.* **84**, 1115–1120.

Fagents, S. A., and L. Wilson 1996. Numerical modeling of ejecta dispersal from transient volcanic explosions on Mars. *Icarus* **67**, 1–18.

Fisher, R. V., and H. U. Schmincke 1984. *Pyroclasitic Rocks*. Springer-Verlag, Berlin/New York.

Francis, P. W., and C. A. Wood 1982. Absence of silicic volcanism on Mars: Implications for crustal composition and volatile abundance. *J. Geophys. Res.* **87**, 9881–9889.

Garvin, J. B., J. J. Frawley, S. E. H. Sakimoto, and C. Schnetzler 2000. Global geometric properties of martian impact craters: An assessment from Mars Orbiter Laser Altimeter (MOLA) digital elevation models. *Lunar Planet. Sci.* **31**, 1619 (abstract).

Geissler, P. E., R. B. Singer, and B. K. Lucchitta 1990. Dark materials in Valles Marineris: Indications of the style of volcanism and magmatism on Mars. *J. Geophys. Res.* **95**, 14,399–14,413.

Gilmore, M. S., J. A. Skinner, and K. L. Tanaka 2001. Crater counts of Noachian surfaces at MOC resolution. *Lunar Planet. Sci.* **32**, 2038 (abstract).

Grant, J. A. 1998. Geologic mapping and drainage morphometry in Margaritifer Sinus, Mars. *Lunar Planet. Sci.* **29**, 1285 (abstract).

Greeley, R., and J. E. Guest 1987. Geologic map of the eastern equatorial region of Mars. U.S. Geol. Surv. Misc. Invest. Series Map I-1802-B.

Gudmundsson, M. T., F. Sigmundsson, and H. Björnsson 1997. Ice–volcano interaction of the 1996 Gjálp subglacial eruption, Vatnajökull, Iceland. *Nature* **389**, 954–957.

Gulick, V. C., and V. R. Baker 1989. Fluvial valleys and martian paleoclimates. *Nature* **341**, 514–516.

Gulick, V. C., and V. R. Baker 1990. Origin and evolution of valleys on martian volcanoes. *J. Geophys. Res.* **95**, 14,325–14,344.

Hartmann, W. K. 1973. Martian surface and crust: Review and synthesis. *Icarus* **19**, 550–575.

Hartmann, W. K. 2001. Martian cratering 7: The role of impact gardening. *Icarus* **149**, 37–53.

Henríquez, F., and R. F. Martin 1978. Crystal-growth textures in magnetite flows and feeder dykes, El Laco, Chile. *Can. Mineral.* **16**, 581–589.

Hoffman, N. 2000. White Mars: A new model for Mars' surface and atmosphere based on CO_2. *Icarus* **146**, 326–342.

Jones, J. G. 1970. Intraglacial volcanoes of the Laugarvatn region, southwest Iceland, II. *J. Geol.* **78**, 127–140.

Jöns, H. P. 1990. Das relief des Mars: Versuch einer zusammenfassenden uebersicht. *Geol. Rundsch.* **79**, 131–164.

Kelsey, C., W. K. Hartmann, J. A. Grier, and D. C. Berman 2000. Observations of a hematite-rich region within Sinus Meridiani. *Lunar Planet. Sci.* **31**, 1524 (abstract).

Kokelaar, P. 1986. Magma–water interactions in subaqueous and emergent basaltic volcanism. *Bull. Volcanol.* **48**, 275–289.

Komatsu, G., P. E. Geissler, R. G. Strom, and R. B. Singer 1993. Stratigraphy and erosional landforms of layered deposits in Valles Marineris, Mars. *J. Geophys. Res.* **98**, 11,105–11,121.

Komatsu, G., J. S. Kargel, V. R. Baker, R. G. Strom, G. G. Ori, C. Mosangini, and K. L. Tanaka 2000. A chaotic terrain formation hypothesis: Explosive outgas and outflow by dissociation of clathrate on Mars. *Lunar Planet. Sci.* **31**, 1434 (abstract).

Lane, M. D., R. V. Morris, and P. R. Christensen 2000. Sinus Meridiani shows spectral evidence for oriented hematite grains. *Lunar Planet. Sci.* **31**, 1140 (abstract).

Lee, P. 1993. Briny lakes on early Mars? Terrestrial Intracrater Playas and Martian Candidates, Abstract for the Workshop on Early Mars: How Warm and How Wet? Lunar Planet. Inst. Tech. Rep. 93–03.

Lucchitta, B. K. 1978. Morphology of chasma walls, Mars. *J. Res. U.S. Geol. Surv.* **6**, 651–662.

Lucchitta, B. K. 1981. Valles Marineris—Faults, volcanic rocks, channels, basin beds. *NASA TM* **84211**, 419–421.

Lucchitta, B. K. 1982. Lakes or playas in Valles Marineris. *NASA TM* **85127**, 233–234.

Lucchitta, B. K. 1990. Young volcanic deposits in the Valles Marineris, Mars. *Icarus* **86**, 476–509.

Lucchitta, B. K. 1998. Pathfinder landing site: Alternatives to catastrophic floods and an Antarctic ice-flow analog for outflow channels on Mars. *Lunar Planet. Sci.* **29**, 1287 (abstract).

Lucchitta, B. K. 1999. Geologic map of Ophir and Central Candor Chasmata (MTM-05072) of Mars U.S. Geol. Surv. Misc. Invest. Series Map I-2568.

Lucchitta, B. K., G. D. Clow, P. E. Geissler, A. S. McEwen, R. A. Schultz, R. B. Singer, and S. W. Squyres 1992. The canyon system on Mars. In *Mars* (H. H. Kieffer, B. M. Jakosky, C. W. Snyder, and M. S. Matthews, Eds.), pp. 453–492. Univ. of Arizona Press, Tucson.

Lucchitta, B. K., N. K. Isbell, and A. Howington-Kraus 1994. Topography of Vallis Marineris: Implications for erosional and structural history. *J. Geophys. Res.* **99**, 3783–3798.

Malin, M. C. 1976. *Nature and Origin of Intercrater Plains on Mars*. Ph.D. thesis, California Institute of Technology, Pasadena.

Malin, M. C., and K. S. Edgett 2000. Sedimentary rocks of Mars. *Science* **290**, 1927–1937.

Masursky, H., J. M. Boyce, A. L. Dial Jr., G. G. Schaber, and M. E. Strobell 1977. Classification and time of formation of martian channels based on Viking data. *J. Geophys. Res.* **82**, 4016–4038.

Max, M. D., and S. M. Clifford 2000. The initiation of martian outflow channels through the catastrophic decomposition of methane hydrate. *Lunar Planet. Sci.* **31**, 2094 (abstract).

McCauley, J. F. 1978. Geological map of the Coprates quadrangle of Mars. U.S. Geol. Surv. Misc. Invest. Series Map I-897.

Murai, I. 1961. A study of the textural characteristics of pyroclastic flow deposits in Japan. *Tokyo Univ. Earthq. Res. Inst. Bull.* **39**, 133–248.

Murchie, S., L. Kirkland, S. Erard, J. Mustard, and M. Robinson 2000. Near-infrared spectral variations of martian surface materials from ISM imaging spectrometer data. *Icarus* **147**, 444–471.

Naslund, H. R., F. M. Dobbs, F. J. Henriquez, and J. O. Nystrom 1997. Irrefutable evidence for the eruption of iron-oxide magmas at El Laco Volcano, Chile. *EOS* **78**, 333.

Naslund, H. R., F. M. Dobbs, F. J. Henriquez, and J. O. Nystrom 1998. Evidence for iron-oxide magmas at El Laco, Chile. *Geol. Soc. Am.* **30**, 91 (abstract).

Nedell, S. S. 1987. Sedimentary geology of the Valles Marineris, Mars, and Antarctic dry valley lakes. *Adv. Planet. Geol.* **89871**, 269–444.

Nedell, S. S., S. W. Squyres, and D. W. Andersen 1987. Origin and evolution of the layered deposits in the Valles Marineris, Mars. *Icarus* **70**, 409–441.

Nelson, D. M., and R. Greeley 1999. Geology of Xanthe Terra outflow channels and the Mars Pathfinder landing site. *J. Geophys. Res.* **104**, 8653–8669.

Neukum, G., and K. Hiller 1981. Martian ages. *J. Geophys. Res.* **86**, 3097–3121.

Noreen, E., K. L. Tanaka, and M. G. Chapman 2000. Examination of igneous alternatives to martian hematite using terrestrial analogs. *Geol. Soc. Am.* **32**, A303 (abstract).

Nummedal, D., and D. B. Prior 1981. Generation of martian chaos and channels by debris flows. *Icarus* **45**, 77–86.

Nyström, J. O., and F. Henríquez 1994. Magmatic features of iron ores of the Kiruna type in Chile and Sweden: Ore textures and magnetite geochemistry. *Econ. Geol.* **89**, 820–839.

Parker, T. J., S. M. Clifford, and W. B. Banerdt 2000. Argyre Planitia and the Mars global hydrologic cycle. *Lunar Planet. Sci.* **31**, 2033 (abstract).

Paterson, W. S. B. 1994. *The Physics of Glaciers*, 3rd ed. Pergamon, Oxford.

Peterson, C. 1981. A secondary origin for the central plateau of Hebes Chasma. *Proc. Lunar and Planet. Sci. Conf.* 12th; *Geochem. Cosmochim. Acta*, 1459–1471.

Peterson, D. W. 1979. Significance of flattening of pumice fragments in ash-flow tuffs. In *Ash Flow Tuffs* (C. E. Chapin and W. E. Elston, Eds.), pp. 195–204. Geol. Soc. Am. Spec. Paper 180. Geol. Soc. Am., Boulder, Co.

Pike, R. J. 1974. Depth/diameter relations of fresh lunar craters: Revision from spacecraft data. *Geophys. Res. Lett.* **1**, 291–294.

Pike, R. J. 1977. Size dependence in the shape of fresh impact craters on the Moon. In *Impact and Explosion Cratering* (O. J. Roddy, R. O. Pepin, and R. B. Merrill, Eds.), pp. 489–510. Pergamon, Elmsford, NY.

Plescia, J. G., and R. S. Saunders 1982. Tectonic history of the Tharsis region, Mars. *J. Geophys. Res.* **87**, 9775–9791.

Presley, M. A., and R. E. Arvidson 1988. Nature and origin of materials exposed in the Oxia Palus—Western Arabia—Sinus Meridiani region, Mars. *Icarus* **75**, 499–517.

Rhodes, A. L., N. Oreskes, and S. Sheets 1997. Recognition of a paleo-hydrothermal system responsible for magnetite formation at El Laco, Chile. *EOS* **78**, 748–749.

Rice, J. W., Jr. 2000. Flooding and ponding on Mars: Field observations and insights from the polar realms of the Earth. *Lunar Planet. Sci.* **31**, 2067 (abstract).

Rotto, S., and K. L. Tanaka 1995. Geologic/geomorphic map of the Chryse Planitia region of Mars. U.S. Geol. Surv. Misc. Invest. Series Map I-2441.

Ruff, S. W., P. R. Christensen, R. N. Clark, H. H. Kieffer, M. C. Malin, J. L. Bandfield, B. M. Jakosky, M. D. Lane, M. T. Mellon, and M. A. Presley 2000. Mars "White Rock" feature lacks evidence of an aqueous origin. *Lunar Planet. Sci.* **31**, 1945 (abstract).

Saunders, R. S. 1979. Geologic map of the Margaritifer Sinus quadrangle of Mars. U.S. Geol. Surv. Misc. Invest. Series Map I-1144.

Schultz, P., R. Schultz, and J. Rogers 1982. The structure and evolution of ancient impact basins on Mars. *J. Geophys. Res.* **87**, 9803–9820.

Schultz, P. H. 1985. Polar wandering on Mars. *Sci. Am.* **253**, 94–102.

Schultz, P. H., and A. B. Lutz 1988. Polar wandering on Mars. *Icarus* **73**, 91–141.

Scott, D. H., and K. L. Tanaka 1982. Ignimbrites of the Amazonis Planitia region of Mars. *J. Geophys. Res.* **87**, 1179–1190.

Scott, D. H., and K. L. Tanaka 1986. Geologic map of the western equatorial region of Mars. U.S. Geol. Surv. Misc. Invest. Series Map I-1802-A.

Sharp, R. P. 1973. Mars—Troughed terrain. *J. Geophys. Res.* **78**(20), 4063–4072.

Skilling, I. P. 1994. Evolution of an englacial volcano: Brown Bluff, Antarctica. *Bull. Volcanol.* **56**, 573–591.

Smellie, J. L. 2000. Lithofacies architecture and construction of volcanoes erupted in englacial lakes: Icefall Nunatak, Mount Murphy, eastern Marie Byrd Land Antarctica. *Spec. Publs. Int. Ass. Sediment.* **30**, 9–34.

Smellie, J. L., and I. P. Skilling 1994. Products of subglacial volcanic eruptions under different ice thicknesses: Two examples from Antarctica. *Sediment. Geol.* **91**, 115–129.

Smith, D. E., and 18 colleagues 1999. The global topography of Mars and implications for surface evolution. *Science* **284**, 1495–1503.

Smith, R. L. 1979. Ash flow magmatism. In *Ash Flow Tuffs* (C. E. Chapin and W. E. Elston, Eds.), pp. 5–28. Geol. Soc. Am. Spec. Pap. 180. Geol. Soc. Am., Boulder, Co.

Spencer, J. R., and F. P. Fanale 1990. New models for the origin of Valles Marineris closed depressions. *J. Geophys. Res.* **95**, 14,301–14,313.

Tanaka, K. L. 1997. Sedimentary history and mass flow structures of Chryse and Acidalia Planitiae, Mars. *J. Geophys. Res.* **102**, 4131–4149.

Tanaka, K. L. 1999. Debris-flow origin for the Simud/Tiu deposit on Mars. *J. Geophys. Res.* **104**, 8637–8652.

Tanaka, K. L. 2000. Dust and ice deposition in the martian geologic record. *Icarus* **144**, 254–266.

Tanaka, K. L., and M. G. Chapman 1992. Kasei Valles, Mars: Interpretation of canyon materials and flood sources. *Proc. Lunar Planet. Sci. Conf.* **22**, 73–83.

Tanaka, K. L., J. S. Kargel, and N. Hoffman 2001. Evidence for magmatically driven catastrophic erosion on Mars. *Lunar Planet. Sci.* **32**, 1898 (abstract).

Theilig, E., and R. Greeley 1979. Plains and channels in the Lunae Planum–Chryse Planitia region of Mars. *J. Geophys. Res.* **84**, 7994–8010.

Van Bemmelen, R. W. 1949. *Geology of Indonesia*. Govt. Printing Office, The Hague.

Van Bemmelen, R. W., and M. G. Rutten 1955. *Tablemountains of Northern Iceland*. Brill, Leiden.

Weitz, C. M. 1999. A volcanic origin for the interior layered deposits in Hebes Chasma. Mars. *Lunar Planet. Sci.* **30**, 1999 (abstract).

Weitz, C. M., and T. J. Parker 2000. New Evidence that the Valles Marineris interior layered deposits formed in standing bodies of water. *Lunar Planet. Sci.* **31**, 1693 (abstract).

Wilhelms, D. E. 1974. Comparison of martian and lunar geologic provinces. *J. Geophys. Res.* **79**, 3933–3941.

Williams, H., and A. R. McBirney 1979. *Volcanology*. Freeman, San Francisco.

Wilson, L., and J. W. Head 1981. Ascent and eruption of basaltic magma on the Earth and Moon. *J. Geophys. Res.* **86**, 2971–3001.

Wilson, L., and J. W. Head 1983. A comparison of volcanic eruption processes on Earth, Moon, Mars, Io, and Venus. *Nature* **302**, 663–669.

Wilson, L., and J. W. Head 1994. Mars: Review and analysis of volcanic eruption theory and relationships to observed landforms. *Rev. Geophys.* **32**, 221–264.

Wise, D. U., M. P. Golombek, and G. E. McGill 1979. Tharsis province of Mars: Geologic sequence, geometry, and a deformation mechanism. *Icarus* **38**, 456–472.

Witbeck, N. E., K. L. Tanaka, and D. H. Scott 1991. The geologic map of the Valles Marineris region, Mars. U.S. Geol. Surv. Misc. Invest. Series Map I-2010.